

Efficient Multi-objective Neural Architecture Search Framework via Policy Gradient Algorithm

Bo Lyu, Shiping Wen

Abstract—Differentiable architecture search has gradually become the mainstream research topic in the field of Neural Architecture Search (NAS) for its high efficiency compared with the early NAS (EA-based, RL-based) methods. Recent differentiable NAS also aims at further improving the search performance and reducing the GPU-memory consumption. However, these methods are no longer naturally capable of tackling the non-differentiable objectives, e.g., energy, resource-constrained efficiency, and other metrics, let alone the multi-objective search demands. Researches in the multi-objective NAS field target this but requires vast computational resources cause of the sole optimization of each candidate architecture. In light of this discrepancy, we propose the *TND-NAS*, which is with the merits of the high efficiency in differentiable NAS framework and the compatibility among non-differentiable metrics in Multi-objective NAS. Under the differentiable NAS framework, with the continuous relaxation of the search space, *TND-NAS* has the architecture parameters (α) been optimized in discrete space, while resorting to the progressive search space shrinking by α . Our representative experiment takes two objectives (*Parameters, Accuracy*) as an example, we achieve a series of high-performance compact architectures on CIFAR10 (1.09M/3.3%, 2.4M/2.95%, 9.57M/2.54%) and CIFAR100 (2.46M/18.3%, 5.46/16.73%, 12.88/15.20%) datasets. Favorably, compared with other multi-objective NAS methods, *TND-NAS* is less time-consuming (1.3 GPU-days on NVIDIA 1080Ti, 1/6 of that in NSGA-Net), and can be conveniently adapted to real-world NAS scenarios (resource-constrained, platform-specialized).

Index Terms—Neural architecture search, reinforcement learning, non-differentiable, supernet

I. INTRODUCTION

NEURAL Architecture Search aims at alleviating the tremendous labor of manual tuning on neural network architectures, which has facilitated the development of AutoML [1]–[3]. Recently, under the fast-growing in this area, NAS models have surpassed previous manually designed models in various research fields. As an intuitive method, Reinforcement Learning (RL) based NAS [4] employs the RNN controller to sample the architecture (represented by sequential indices), and the validation accuracy of each candidate architecture is viewed as the reward for policy-gradient optimization. Although relying on the “performance ranking hypothesis” (confirmed by statistical experiments in MdeNAS [5]) to accelerate, in the RL-based NAS route, retraining from scratch of each architecture is inevitable. Thus a mass of computational

This publication was made possible by NPRP grants: NPRP 8-274-2-107 from Qatar National Research Fund. The statements made herein are solely the responsibility of the author[s]. (*Corresponding author: Shiping Wen*.)

B. Lyu is with School of Computer Science and Engineering, University of Electronic Science and Technology of China (email: blyucs@outlook.com). S. Wen and Z. Yan are with Australian AI Institute, Faculty of Engineering and Information Technology, University of Technology Sydney, Ultimo 2007, Australia (email: {shiping.wen; yan.zheng}@uts.edu.au).

overhead (electricity cost, time cost) is required (20,000 GPU-days in [4] and 2,000 in [6]), which has beyond the reach of ordinary research institutes and commercial organizations. So some subsequent literature try to promote the efficiency of the search procedure, e.g. ENAS [7]. However, due to the efficiency issue, less research attention is addressed on the RL-based NAS approaches after the rise of differential NAS [8].

By continuous relaxation of the search space, differentiable NAS researches make the loss function differentiable w.r.t architecture weights, thus the search can be processed directly by gradient-based optimization. Benefits from the weight-sharing of different candidate architectures that come from the unified supernet [9]–[11], it saves the unnecessary time-cost and computation-consumption that are resulted from the candidate model’s sole training from scratch. Even with high search efficiency, differentiable NAS researches rarely involves the non-differentiable objectives, e.g., energy, latency, or memory consumption, and multi-objective are merely jointly considered.

Parallel to the explosive development of the differentiable NAS sub-field, the multi-objective NAS methods (MnasNet [12], DPP-Net [13], MONAS [14], Pareto-NASH [15], [16], [17]) dedicate to searching for the neural architectures in discrete space with the consideration of multi-dimensional metrics, including differentiable and non-differentiable ones. There is no doubt that the computational overhead of the multi-objective NAS is huge.

Our method relies on the differentiable NAS as the main search framework, in which candidate operations are progressively eliminated base on the architecture parameters α after each stage of the search, in the meantime, the depth of the model is increased gradually [18]. The difference is that we detach the architecture parameter α from the gradient descend framework and formulate the training as an optimization problem in discrete space by the reinforcement learning algorithm. In this way, the non-differentiable metrics can naturally be involved in the search process. Generally, our work jointly searches the architectures across the differentiable and non-differentiable metrics, it combines the merits of both differentiable NAS and multi-objective NAS. We name our search framework as “TND-NAS”, the overall structure is illustrated in Fig. 1. Though under differentiable NAS framework, *TND-NAS* has the architecture parameters (α) been optimized in discrete space, and resort to the progressive search strategy by α to shrink the search space.

Our contributions may be summarized as follows:

1. Our proposed *TND-NAS* methods is capable to tackle

the non-differentiable objectives under the differentiable search framework, that is, with the merits of high efficiency in differentiable NAS and the objective compatibility of multi-objective NAS.

2. We comprehensively address the “optimization gap”, “depth gap” issues, as well as the “GPU-memory consumption” issue in our search. Our search process is also end-to-end, that is, without any skip-connection dropout and compulsive restriction of node indegree.

3. Through flexible and customized search configurations, the visualization of architecture evolving during the search process show that our method can reach the trade-off among differentiable and non-differentiable metrics.

II. RELATED WORK

RL/EA-based NAS. Traditional architecture search methods start from employing Evolutionary Algorithm (EA) as the search strategy [17], [19]–[24]. In these works, high-performing network architectures are mutated, and less promising architectures are discarded. Recently, the significant success of RL-based NAS is first reported by [4], [6]. These works provide remarkable results on CIFAR-10 and PTB datasets, but require excessive computational resources. ENAS [7] comes in the continuity of previous work [4], [6], it proposes the weight-sharing strategy to significantly improve the searching efficiency. Overall, the RL/EA-based NAS methods search the architecture over a discrete domain and suffer from the efficiency issue.

Differentiable NAS. By continuous relaxation of the search space, DARTS [8] constructs the supernet by mixed-edge operation, the task of architecture search is treated as learning a set of continuous architecture parameters. Thus the objective of “searching for the architecture to obtain the best *Accuracy*” is formulated as a bilevel optimization problem with α as the upper-level and ω as the lower-level. In this way, the NAS method is greatly improved in terms of search efficiency. DARTS and the followed works also suffer from the high GPU-memory overhead issue [25], which grow linearly w.r.t. candidate-set size. As a result, these works have to search with only a few blocks (cells), but evaluate the architecture with more blocks stacked, which undoubtedly brings in the “depth gap” issue [18]. Meanwhile, DARTS does not take into consideration the non-differentiable metrics (e.g. *FLOPs*, *Latency*), for these metrics are different from the *Accuracy* that has the cross-entropy function as its differentiable objective function [26]. Motivated by DARTS and dedicated to reconciling the “depth gap” and “GPU-memory consumption” issues, P-DARTS [18] introduces the progressive NAS which evolves the supernet from a shallow-wide one to a deep-narrow one. ProxylessNAS [27] also employs continuous relaxation in DARTS and try to directly search without proxy-task (targeting the “proxy-task gap”). And benefit from the regularity of pre-defined chain-style structures, ProxylessNAS constructs *inference latency* expectation of each chain-style layer by accumulating each layer’s predicted latency value, and formulating it as the regularization item. This makes *inference*

latency metric differentiable, thus the bi-objective problem may be optimized uniformly. Whereas the pre-defined chain-style network limits its search space and results in expensive GPU memory and time cost. Further, for the non-chain-style backbone, method in ProxylessNAS is not feasible to tackling the *Latency*, *FLOPs*, and *Parameters*, as these metrics cannot be calculated by the linear transformation function.

Multi-objective NAS and Platform-aware NAS. Multi-objective NAS methods (MnasNet [12], MONAS [14]) concentrate on searching the architectures with consideration of multi-dimensional evaluation metric, and In these researches, model’s consumption (Parameters, FLOPs, Latency, Energy) are jointly employed to formulate the reward-penalty coefficients of the *Accuracy* [28]. Through the optimization of the single-policy multi-objective reinforcement learning algorithm, the search process is prone to emit the candidate architectures that reach the trade-off among these contradictory metrics. DPP-Net [13] proposed the progressive search methods that involve device-aware characteristics, including QoS (Quality of Service) and hardware resource requirements (e.g., memory size), which are critical metrics of the deployment of deep neural network. It also takes into consideration the different target platforms, e.g. workstations, mobiles, and embedded devices. In LEMONADE [29], an evolutionary algorithm is proposed to address the multi-objective NAS. It achieves state-of-the-art Pareto-optimal performance on CIFAR10. Critically, these multi-objective NAS methods are based on reinforcement learning or evolutionary algorithms, so their disadvantages in search efficiency are obvious, e.g., LEMONADE [29] consumes 80 GPU-days. Also, dedicating to the customized NAS, some platform-aware methods [30] are proposed, as well as the method that is specified for the resource-constrained situation [31].

One-shot NAS. One-shot NAS researches [9], [10], [32] construct the search space into a unified supernet, from which sub-architectures are solely sampled and evaluated, and these sub-architectures share the common weights of the supernet (directly inherited). Before the sampling in one-shot NAS, the supernet is trained uniformly without any bias to any sub-networks, but intuitively, a well-trained supernet does not always produce the best-performance sub-network. This brings up the “optimization gap” between the sub-networks and supernet. As is discussed in [26], “optimization gap” means that a well-optimized super-network does not necessarily produce well-performance sub-architectures, whereas this is exactly what the conventional supernet-based NAS method adopts.

III. METHODOLOGY

A. Preliminary

Our search strategy basically follows differentiable NAS. To make the search space continuous, the operation o in specified location (i, j) is characterized by all candidate operations in \mathcal{O} , as Eq. (1):

$$\bar{o}^{(i,j)}(x) = \sum_{o \in \mathcal{O}} \frac{\exp(\alpha_o^{(i,j)})}{\sum_{o' \in \mathcal{O}} \exp(\alpha_{o'}^{(i,j)})} o(x) \quad (1)$$

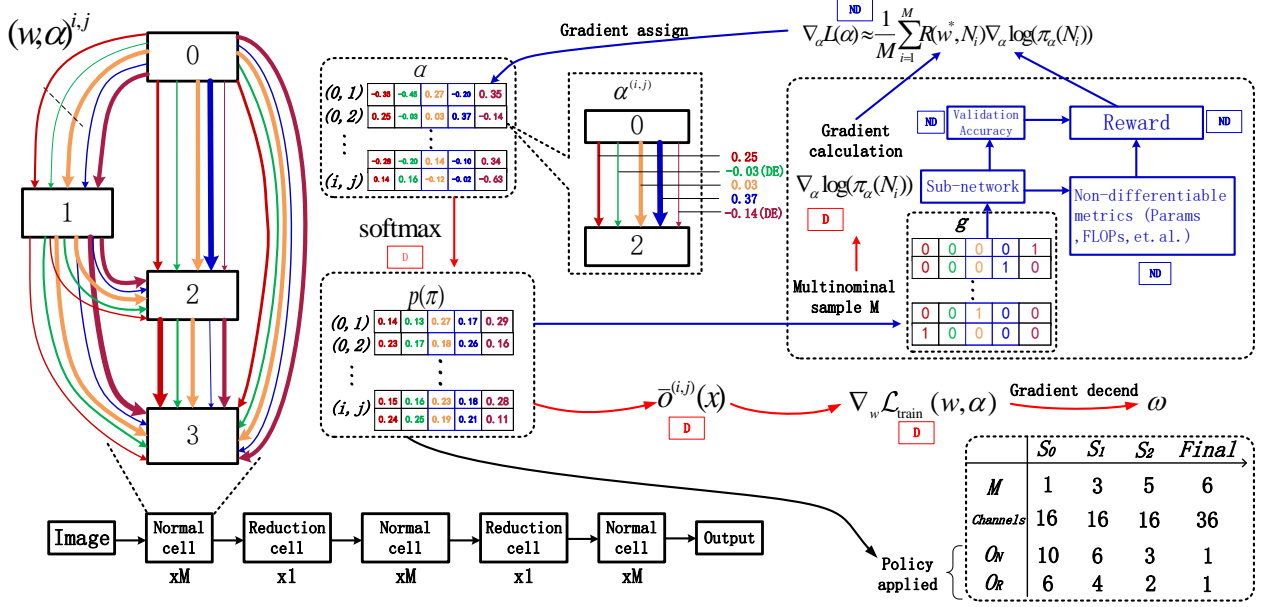


Fig. 1. Illustration of the overall framework of TND-NAS. Our baseline follows the progressive differentiable NAS framework, including macro-structure, micro-structure, and the progressive search. The search space of the normal/reduction cell can be represented by a directed acyclic graph (DAG). The training of the architecture in our framework is separated from the differentiable framework to deal with non-differentiable optimization objectives. For clarity, the red forward route, marked by the red “D”, represents a computation graph is differentiable w.r.t (ω, α) , whereas the blue forward route with the blue “ND” means the computation graph is non-differentiable w.r.t (ω, α) .

where the mixed operation for a pair of nodes (i, j) are parameterized by a vector $\alpha^{(i,j)}$ with dimension $|\mathcal{O}|$. Obviously, the task of architecture search then is to learn a set of continuous variables. Thus NAS procedure is formulated as a bilevel optimization problem with α as the upper-level variable and ω as the lower-level variable, as shown in Eq. (2).

$$\begin{aligned} \min_{\alpha} \quad & \mathcal{L}_{val}(w^*(\alpha), \alpha) \\ \text{s.t.} \quad & w^*(\alpha) = \arg \min_{\alpha} \mathcal{L}_{train}(w, \alpha) \end{aligned} \quad (2)$$

To effectively solve this bilevel optimization problem, DARTS approximates the solution by alternate optimization, as is presented in Algorithm 1.

Algorithm 1: DARTS

Create a mixed operation $\bar{o}^{(i,j)}$ parametrized by $\alpha^{(i,j)}$ for each edge (i, j) ;

while *TRUE* **do**

- 1. Update α by $\mathcal{L}_{val}(w, \alpha)$
- 2. Update ω by descending $\nabla_w \mathcal{L}_{train}(w, \alpha)$

end

Deriving the final architecture based on the learned α

Base on DARTS, the promising improvement of P-DARTS is the progressive search strategy, which is divided into three stages, gradually evolving from a shallow-wide supernet to the final deep-narrow supernet. This strategy not only solves the “depth gap” problem but also reduces the GPU-memory consumption and improves the search efficiency.

B. Search method

We describe TND-NAS in detail in this section. According to the customs, under the supernet framework, we take w to stand for the weight parameters, and α to represent the architecture parameters. As shown in Fig. 1, the search process is formulated as bilevel optimization problem w.r.t α and ω . During the search, TND-NAS resorts to the continuous relaxation of the search space, the progressively shrinking of the candidate operations (presented as the “search space approximation” in [18]), and first-order approximation of differentiable NAS in Algorithm 1. Importantly, the architecture parameters α are not directly trained by gradient descent with differentiable loss function (cross-entropy loss), but rather trained by reinforcement learning (REINFORCE [33]) in discrete space, which follows the non-differentiable route (marked blue in Fig. 1). Whereas we keep the optimization of ω in the differentiable route (marked red in Fig. 1).

1) *Training of weights w*: Commonly, the supernet is constructed by the stack of mixed-edge operation o , the calculation is presented in Eq. (1). In terms of the weight parameters training, w is optimized by the gradient descent of cross-entropy loss:

$$w^*(\alpha) = \arg \min_w \mathcal{L}_{train}(w, \alpha) \quad (3)$$

2) *Sampling architectures by α* : In terms of the architecture sampling, for each index (i, j) , $p^{(i,j)}$ is calculated by softmax of $\alpha^{(i,j)}$, the binary vector $g^{(i,j)}$ is sampled by multinomial distribution with probability vector $p^{(i,j)}$.

$$p^{(i,j)} = \text{softmax}(\alpha^{(i,j)}) \quad (4)$$

$$g^{(i,j)} \sim \text{Multi}(p^{(i,j)}, 1) \quad (5)$$

the sub-network structured by g inherits the supernet's weight parameters:

$$N_m = \mathcal{A}(g_m) \quad (6)$$

where N stands for the sub-network, \mathcal{A} represents the supernet, and m is the sampling index.

3) *Optimized by REINFORCE*: Further, the neural architecture search procedure is formulated as the optimization of α to achieve the optimal reward (R) of the architectures assembled with the binary gate of g :

$$\begin{aligned} \alpha^* &= \arg \max_{\alpha} \mathcal{J}_{\text{val}}(w^*, \alpha) \\ &= \arg \max_{\alpha} \mathbb{E}_{g \sim \alpha}(R_{\text{val}}(w^*, N_g)) \end{aligned} \quad (7)$$

where \mathcal{J} is the optimization objective function, which is represented by the expectation of the reward achieved by the sub-networks.

From the perspective of RL, we raise the correspondence between NAS scenarios and reinforcement learning concepts, as shown in Table I. It can be concluded that due to the differ-

TABLE I
NOTATION IN RL AND THE CORRESPONDING MEANING IN TND-NAS SCENARIOS.

Notation in RL	Definition in TND-NAS
Environment (e)	Supernet
Environment change	Evolving of the supernet (α, ω)
Reward (R)	Sampled architecture's evaluation metrics
Policy (π)	p from architecture parameters α
Action (a)	Sampling candidate architectures (with weights) by policy (π)
Policy applied	Shrinking the search space

ences between the sampling strategy and the applied strategy, this problem can be viewed as an off-policy reinforcement learning problem. We empirically resort to the REINFORCE with baseline [33], in the process of gradient ascent, the gradient is estimated by sampling, that is:

$$\begin{aligned} \nabla_{\alpha} \mathcal{J}_{\text{val}}(\alpha) &= \mathbb{E}_{N \sim \pi_{\alpha}(N)}[R_{\text{val}}(w^*, N) \nabla_{\alpha} \log(\pi_{\alpha}(N))] \\ &\approx \frac{1}{M} \sum_{m=1}^M (R_{\text{val}}(w^*, N_m) - b) \nabla_{\alpha} \log(\pi_{\alpha}(N_m)) \end{aligned} \quad (8)$$

where M is the sample number of candidate architectures in one iteration. The baseline function is utilized to reduce the variance to reach the unbiased estimation of gradient, in which b is the moving average of the previous architecture rewards. As aforementioned, multinomial sampling is employed to reach the trade-off between exploit and exploration, to avoid the permanent dominance of one operation branch from the beginning. In other words, if argmax is employed for sampling, it is easy to lead to the lack of exploration and fall into the local optimal solution.

4) *Reward calculation*: Apparently, in terms of performance, the most common metric *Accuracy* can be directly employed as a reward. Much more attention needs to be addressed to the multi-objective scenario, in which the reward function needs to be designed based on real-world requirements. For example, resource-constrained scenarios need the trade-off between performance and efficiency, e.g., memory consumption (mode size and number of accesses), or inference latency. Motivated by Mnasnet [12], taking the *Accuracy* and *Parameters* as the objectives, we make the reward be linearly w.r.t *Accuracy*, but non-linearly w.r.t *Parameters*, which is treated as a reward-penalty factor in the non-linearly scalarization function, presented in Eq. (9). The reward function surface is shown in Fig. 2, in which the cross-section curves (under one specific metric) and the corresponding projection curves are also plotted to present the reward-penalty mechanism.

$$R = \text{Acc} \cdot \left(\frac{\text{Params}}{P} \right)^{\beta} \quad (9)$$

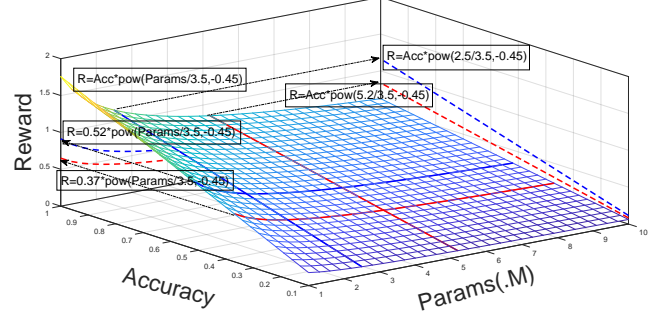


Fig. 2. The surface of the reward function in Eq.(9). The spatial curves under specific *Parameters* and *Accuracy* (keep consistent) and their projection lines are shown, respectively. The image arrows indicate the projection orientation.

In this way, the non-differentiable metrics can naturally be involved in the search process by a scalarization function f that transform the reward vector to a scalar one (single-policy MORL [34]–[36]). In the multi-objective situation, intuitively, the scalarization function can be modified, e.g. *Accuracy*, *Parameters*, and *Latency*, as Eq. (10) shows.

$$R = \text{Acc} \cdot [a \cdot \left(\frac{\text{Params}}{P} \right)^{\beta} + c \cdot \left(\frac{\text{Latency}}{L} \right)^{\gamma}] \quad (10)$$

where P, L are the reward-penalty reference of *Parameters*, and *inference latency*, respectively. β and γ are the corresponding reward-penalty coefficient, and a, c is the weights, subject to $a + c = 1$.

5) *Progressively deriving the architecture*: We primarily follow the main search framework of P-DARTS, which has the searched architecture gradually decreased by “search space approximation and regularization”. The search space is shrunk by Eq. (11):

$$O_{k+1}^{(i,j)} = O_k^{(i,j)} - O_k^{(i,j)}(\text{argmin}(p^{(i,j)}, n_k)) \quad (11)$$

where n_k is the decreased number of candidate-set size in each stage, k indicates the stage and $k \geq 0$, $n_0 = 4$, $n_1 = 3$,

$n_2 = 2$ in our setting. Similarly, the whole layer number of the network is increased by Eq. (12):

$$L_{k+1} = L_k + l_{k+1} \quad (12)$$

where $k \geq 0$ and $L_0 = 5$, $l_1 = 7$, $l_2 = 15$ in our setting.

We present the overall search method of TND-NAS in Algorithm 2.

Algorithm 2: TND-NAS

```

for  $k = 0 \rightarrow stage\_num - 1$  do
  Create a mixed operation
   $\bar{o}_k^{(i,j)} \in O_k^{(i,j)}$  parametrized by  $\alpha_k^{(i,j)}$ 
  for each edge  $(i, j)$ ;
  Increase layer number  $L_k$  by Eq. (12);
  Construct the supernet by  $\bar{o}_k^{(i,j)}$  and  $L_k$ ;
  for  $epoch = 0 \rightarrow num\_epoch - 1$  do
    for  $step = 0 \rightarrow train\_step$  do
      if  $epoch > e_k$  then
        /*Pre-training for  $e_k$ 
        epochs*/
        if  $step \% rl\_interval == 0$  then
          | Update architecture  $\alpha$  by Eq. (8)
        end
      end
      Update weights  $\omega$  by Eq. (3)
    end
  end
  Shrinking each  $O_k^{(i,j)}$  by Eq. (11);
end

```

Deriving the final architecture.

IV. RELATIONSHIP AND COMPARISON WITH PRIOR WORKS

The premise of all pure *RL-based or EA-based NAS* is the “performance ranking hypothesis”, and the performance identification of the candidate architecture is conducted through the training by fewer epochs on proxy-tasks. Even though, the independent training from scratch one-by-one inevitably brings a huge amount of computation.

DARTS solves the time-consuming problem in search, it brings up the GPU memory consumption problem and the “depth gap” issue. *P-DARTS* introduces the progressive NAS to tackle the “depth gap” issue, but there still exist the following issues:

1. The search procedure is not end-to-end, that is:
 - i. The search model is processed in one initial channels setting, but evaluated in another setting.
 - ii. The skip-connection is directly restricted in the final stage.
 - iii. The indegree of one node is compulsively limited by 2 when deriving the final architecture.
- These issues inevitably bring the “gaps” between the searched architectures and the evaluation architectures, we may call it the “architecture inconsistent gap”.
2. Similar with *DARTS*, *P-DARTS* is not capable of optimizing the non-differentiable objectives e.g. *Parameters*, *FLOPs*, let

TABLE II
CHARACTERISTICS COMPARISON WITH THE STATE-OF-THE-ART NAS METHODS.

	NASNet	MNASNet	DARTS	FBNet [38]	ProxylessNAS	P-DARTS	TND-NAS
Differentiable metrics	✓	✓	✓	✓	✓	✓	✓
Non-differentiable metrics	✗	✓	✗	✗	✗	✗	✓
Low GPU-memory	✓	✗	✗	✓	✓	✓	✓
Low time cost	✗	✗	✓	✗	✓	✓	✓

alone achieving the trade-off between model efficiency and performance, as is demonstrated in Section VI-C. Our method improves the *P-DARTS* framework and inherits its progressive shrinking strategy. However, there are two essential differences:

i. The training of the architecture parameters α in our method is reinforcement learning in discrete space, which is separated from the differentiable NAS framework, so as to deal with the non-differentiable metrics.

ii. We adopted the end-to-end search to compensate for the “optimization gap” in *P-DARTS*.

Towards the “proxy-task performance gap”, *ProxylessNAS* proposes the search without proxy-task by a pre-defined chain-style network (MobileNetV2 [37]). But the search space in this work is limited (the feature fusion across the cells that are not adjacent is not performed), the GPU-consumption is also dramatical. Crucially, the method to handle non-differentiable metrics proposed in *ProxylessNAS*, accumulating the *latency* expectation as the regularization item, is not feasible for the non-chain-style search space (DARTs-like, NAS-RL, NASNet) [26].

For clarity, we summarize the comparisons of metrics and main property of the state-of-the-art NAS methods/framework in Table. IV.

V. EXPERIMENTS

A. Datasets

Our search and training processes are conducted on 2 popular image classification datasets, CIFAR10 and CIFAR100 [39], which both have 50K images for training and 10K images for testing. The images are all scaled to the same resolution of 32×32 and uniformly labeled over 10/100 classes. During the search procedure, we keep the training set split into two equal-size subsets, one for weight-parameters (ω) training and the other for architecture (α) validation. But in full training, we resort to the regular splitting of train/test.

B. Architecture Search

1) *Experimental setting*: We conduct our experiments using PyTorch 1.4 framework on 2 NVIDIA 1080Ti GPUs that each with 11GB memory. Our search hyper-parameters are presented in Table. III. For clarity, our illustration experiment only aims at the optimization of the *Accuracy* and *Parameters*, the RL reward follows Eq. (9).

TABLE III
HYPER-PARAMETERS OF SEARCH.

Batch size	128	Initial channels	24
Total epochs	25	Layers	5,12,20
Pretrain epochs	10	Drop operation num	4,3,2
Optimizer (ω)	SGD	Weight decay	4e-5
LR	0.025	LR decay	cosine
Momentum	0.9	Reference of Params	4.4,3.2,1.8
Dropout ratio	0.3	Penalty coefficient(C10)	-0.60,-0.60,-0.60
Optimizer (α)	Adam	Penalty coefficient(C100)	-0.75,-0.85,-0.85
RL interval	1(each)	RL sampling batch size	10

2) *Search space*: In terms of the predefined backbone of the search space, we follow the DARTS/P-DARTS, but as for the operations set, we make slight adjustments.

Normal cell:

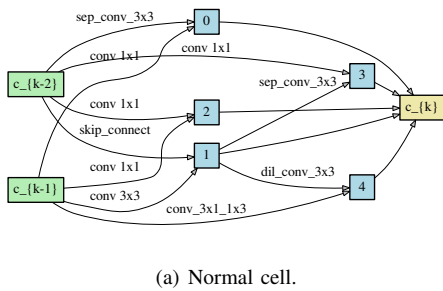
- none
- skip_connect
- sep_conv_3x3
- conv 1x1
- conv_3x1_1x3
- sep_conv_5x5
- sep_conv_7x7
- dil_conv_3x3
- conv 1x1
- conv 3x3

Reduction cell:

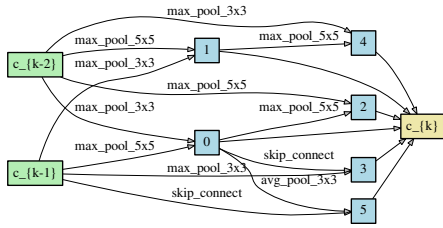
- none
- skip_connect
- max_pool_3x3
- avg_pool_3x3
- max_pool_5x5
- max_pool_7x7

So the search space of TND-NAS is $14^{10} \times 14^6 = 2 \times 10^{18}$, where 14 is the mixed-edge number of DAG.

3) *Search results*: Our searched normal cell's visualization is shown in Fig. 3(a), and reduction cell is shown in Fig. 3(b). Our search process costs merely 0.65 days on 2 NVIDIA 1080Ti GPU, each with only 11G memory. Compared with previous promising multi-objective NAS methods, our method achieves a substantial improvement in search resource cost (1.3 GPU-days).



(a) Normal cell.



(b) Reduction cell.

Fig. 3. The searched result (CIFAR10-S) of TND-NAS. The *Parameters* of this architecture is 1.09M with 16 initial channels.

TABLE IV
SEARCH COST COMPARISON WITH STATE-OF-THE-ART MULTI-OBJECTIVE NAS METHODS.

Methods	Search strategy	Search cost
MONAS [14]	RL	/
MnasNet [12]	RL	4.5 days on 64 TPUv2
LEMONADE [29]	EA	80 GPU days
DPP-Net [13]	SMBO	8 GPU days on 1080Ti
PARETO-NASH [15]	EA	56 GPU days
lu2019nsga	EA	8 GPU days on 1080Ti
TND-NAS	gradient+RL	1.3 GPU days on 1080Ti

4) *Results analysis*: Benefits from the end-to-end search (the searched architectures are directly evaluated with full training from scratch), our normal/reduction cell architecture takes on a more heterogeneous form. The indegree of one node is not limited, and skip-connections are not restricted constrainedly, and all edges are removed in DAG only in case of the “none” operation is selected. From Fig. 3, the deep connection is preserved, and *conv 1 × 1* is frequently selected for its compact in *Parameters* and the ability of feature fusion among channels of the feature map.

C. Architecture Evaluation

1) *Training details*: Our training details follow the experimental setting of evaluation in P-DARTS, evaluation training hyperparameters are shown in Table. V.

TABLE V
HYPER-PARAMETERS OF EVALUATION.

Batch size	128	Initial channels	24
Epochs	600	Layers	20
Optimizer	SGD	Weight decay	3e-4
Learing rate	0.025	LR decay	cosine
Momentum	0.9	Dropout ratio	0.3
Auxiliary towers weight	0.4	Cutout regularization len	16

2) *Evaluation on CIFAR10 and CIFAR100*: For comparison, some state-of-the-art approaches are listed in Table. VI, including the manually designed models and outstanding NAS models. Our experiment reaches a series of scalable models on CIFAR10: extremely compact model (S) of 3.3% test error with 1.09M Parameters, moderate model (M) of 2.7% with 3.2M Parameters, and large model (L) of 2.54% with 9.57M Parameters, which has shown the flexibility of TND-NAS. Our search experiment on CIFAR100 also achieves the promising results: 18.3% test error with 2.46M Parameters (S), 16.73% with 5.46M Parameters (M), 15.2% with 12.88M Parameters (L). As demonstrated, TND-NAS is comparable with the P-DARTS, but much more diversified in model scale. As for the search time cost, our TND-NAS is slightly more time-consuming than P-DARTS, but much more efficient than the RL/EA-base NAS methods.

VI. ABLATION AND DIAGNOSTIC EXPERIMENTS

A. Effect of search algorithm

1) *Reinforcement of performance*: First, we verify the effectiveness of the search algorithm on the differentiable metric.

TABLE VI
COMPARISON OF THE EVALUATION RESULTS.

Architecture	Test Err. (%)		Params (M)	Search Cost (GPU-days)	Search Method
	C10	C100			
DenseNet-BC [40]	3.46	17.18	25.6	-	manual
NASNet-A + cutout [6]	2.65	-	3.3	1800	RL
AmoebaNet-A + cutout [23]	3.34	-	3.2	3150	evolution
AmoebaNet-B + cutout [23]	2.55	-	2.8	3150	evolution
Hierarchical Evolution [24]	3.75	-	15.7	300	evolution
PNAS [41]	3.41	-	3.2	225	SMBO
ENAS + cutout [7]	2.89	-	4.6	0.5	RL
DARTS (first order) [8]	3	17.76	3.3	1.5	gradient-based
DARTS (second order) + cutout [8]	2.76	17.54	3.3	4	gradient-based
SNAS + mild constraint + cutout [42]	2.98	-	2.9	1.5	gradient-based
SNAS + moderate constraint + cutout [42]	2.85	-	2.8	1.5	gradient-based
SNAS + aggressive constraint + cutout [42]	3.1	-	2.3	1.5	gradient-based
ProxylessNAS + cutout [27]	2.08	-	5.7	4	gradient-based
P-DARTS CIFAR10 + cutout [18]	2.5	16.55	3.4	0.3	gradient-based
P-DARTS CIFAR100 + cutout [18]	2.62	15.92	3.6	0.3	gradient-based
P-DARTS CIFAR10 (large) + cutout [18]	2.25	15.27	10.5	0.3	gradient-based
P-DARTS CIFAR100 (large) + cutout [18]	2.43	14.64	11	0.3	gradient-based
TND-NAS CIFAR10 (S) + cutout	3.3	-	1.09	1.3 [†]	gradient + RL
TND-NAS CIFAR10 (M) + cutout	2.70	-	3.2	1.3 [†]	gradient + RL
TND-NAS CIFAR10 (L) + cutout	2.54	-	9.57	1.3 [†]	gradient + RL
TND-NAS CIFAR100 (S) + cutout	-	18.3	2.46	1.3 [†]	gradient + RL
TND-NAS CIFAR100 (M) + cutout	-	16.73	5.46	1.3 [†]	gradient + RL
TND-NAS CIFAR100 (L) + cutout	-	15.20	12.88	1.3 [†]	gradient + RL

[†] Performed on 2 Nvidia 1080Ti GPU each with 11G memory for 0.65 day

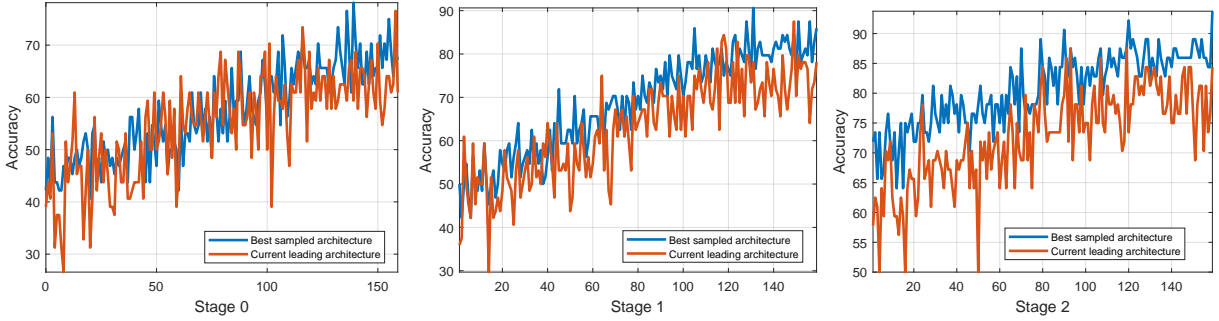


Fig. 4. Reinforcement effect of searching for the best-performance architecture. The $\max(\text{Acc}(\mathcal{A}(g)))$ and $\text{Acc}(\mathcal{A}(\text{argmax}(\alpha)))$ increase synergistically.

Taking validation *Accuracy* as the single reward of reinforcement learning, we monitor two indicators during the search process at each stage, one is the $\max(\text{Acc}(\mathcal{A}(g)))$, in which, $g^{(i,j)} \sim \text{Multi}(\pi^{(i,j)}, 1)$, the other is $\text{Acc}(\mathcal{A}(\text{argmax}(\alpha)))$. As can be seen from Fig. 4, the two precision values are continuously improved, which reflects the effectiveness of the algorithm in effectively searching out the architectures with excellent precision performance.

2) *Reinforcement of Parameters*: Additionally, we explore the perception and discrimination ability of the search algorithm for non-differentiable metrics. Take the *Parameters* as an example, we only have *Parameters* as the reward to search for the architecture that of maximum *Parameters* or minimum *Parameters*. It can be seen that to achieve the best accuracy, the search tends to adopt all “conv_3 × 3” convolution, and the final index converges to “conv_3 × 3” operation.

B. Effect of the model compression without performance sacrifice

We further focus on the effect of the search that incorporates the metrics of accuracy and computational cost. Our experiment performs the comparison between two different penalty coefficients (0 and -0.25) by tracking the *Parameters* and *Accuracy*. It can be seen that, in the experiment with penalty coefficients of 0, the *Parameters* and *Accuracy* values increase synergistically, which can be interpreted as that the increase in *Accuracy* at the cost of the increase in *Parameters*. However, after employing the reward-penalty mechanism (with penalty coefficients of -0.25), while the *Parameters* are maintained and the accuracy is still enhanced.

C. Comparison with P-DARTS during search

We will experimentally and analytically compare our method with P-DARTS in several aspects.

1. We experimentally found that the compactness of models

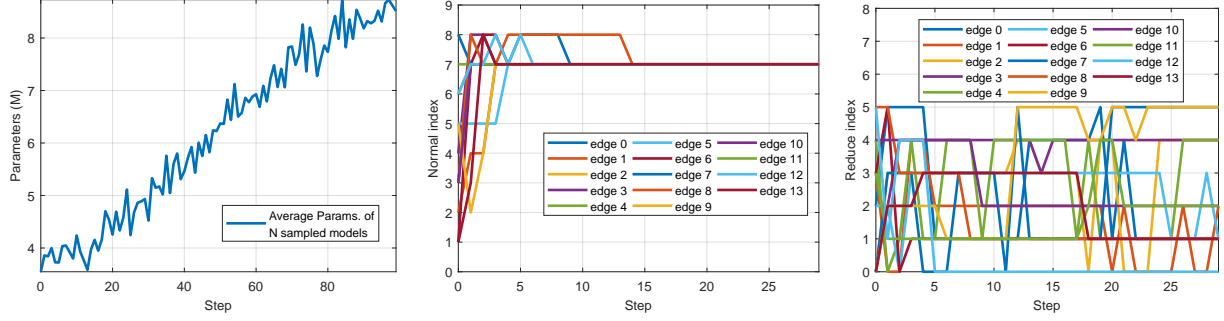


Fig. 5. Reinforcement effect to search for the maximum *Parameters* architecture. The average *Parameters* of the sampled models continuously increase, the Normal cell architecture that determine the *Parameters* also converges to regular “conv 3×3 ” operation (represented by operations index 7)

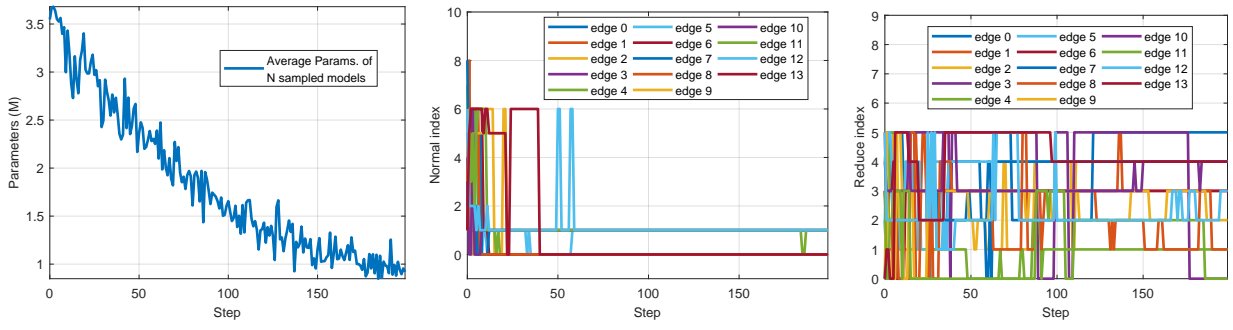


Fig. 6. Reinforcement effect of searching for the minimum *Parameters* architecture. The average *Parameters* of the sampled models continuously decrease, the Normal cell architecture that determine the *Parameters* also converges to *skip_connection* (index 1) and *none* operation (index 0)

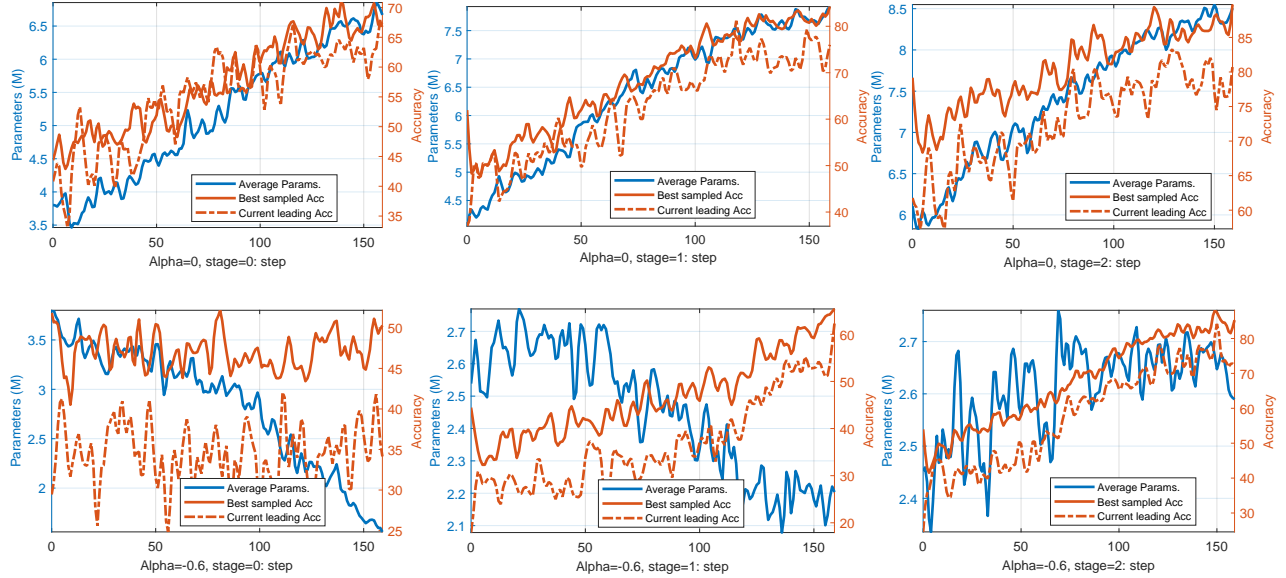
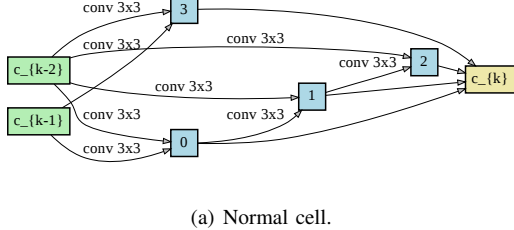


Fig. 7. Effect of the model compression without performance sacrifice, following the reward presented in Eq.(9). Top: penalty coefficients of 0, the increase in *Accuracy* at the cost of the increase in *Parameters*. Bottom: penalty coefficients of -0.25, the *Parameters* are maintained, but the *Accuracy* is still enhanced.

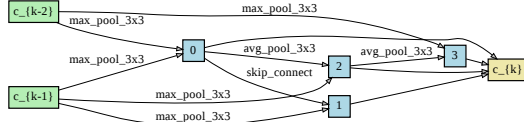
in P-DARTS benefits from the compact operation in the search space. Still using *Parameters* as an example, we add “conv₃ × 1₁ × 3”, “conv₃ × 3” to the original search space of P-DARTS, then the *Parameters* of the obtained model will reach 8.11M when channel is 36 (end-to-end without stripping or restricting).

2. We believe that the promising performance of P-DARTS benefits from the predefined backbone structure. In this regard, two validation experiments are conducted, results presented in Table. VII:

i. We initialize the network’s normal cell with all regular “conv₃ × 3” convolutions (keep the same reduce cell), as is

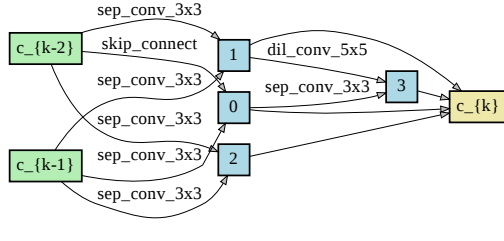


(a) Normal cell.

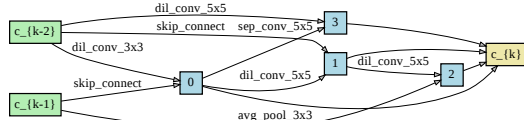


(b) Reduction cell.

Fig. 8. Intentionally designed representative architectures. Top: Normal cell with all $conv_{3 \times 3}$. Bottom: Reduction cell, keep the reduction architecture of P-DARTS.



(a) Normal cell.



(b) Reduction cell.

Fig. 9. The randomly initialized architecture, including normal cell and reduction cell.

TABLE VII
PERFORMANCE INVESTIGATION OF P-DARTS.

Arch	Params	Performance
Intentionally designed representative architectures (Fig. 8)	12.1M	97.5%
Randomly initialized architecture (Fig. 9)	3.97M	97.25%

illustrated Fig. 8. Under the recommended experimental setting (hyperparameters) of P-DARTS, the full training precision is 97.5%; ii. Based on the current search space we tried to manually write a random network (as Fig. 9 shows), finally it still achieves a relatively promising accuracy of 97.25%. That is, the architecture search that is only towards precision is not very meaningful, instead, the search with consideration of other metrics or customized requirements, to reach the trade-

TABLE VIII
END-TO-END COMPARISON OF P-DARTS AND TND-NAS.

	In-degree of Node	Restrict skip-connection	Operation scale limit	Layer gap
P-DARTS	✓	✓	✓	✓
TND-NAS	✗	✗	✗	✗

off is more meaningful.

3. It is unreasonable for P-DARTS to constrainedly restrict the skip-connection number and the indegree of the DAG nodes in the final stage.

To sum up, the comparisons between the TND-NAS and P-DARTS in the search pipeline are listed in Table. VIII. TND-NAS abandons the aforementioned restrictions and manual intervention in the search pipeline of P-DARTS, to achieve end-to-end search.

VII. CONCLUSION

This work incorporates the differentiable NAS framework with the capability to handle non-differentiable metrics, and aims to reach the trade-off among non-differentiable and differentiable metrics. Meanwhile, our method reconciles the merits of multi-objective NAS and differentiable NAS and is feasible to be applied in the real-world NAS scenarios, e.g. resource-constrained, and platform-specialized. Taking the *Parameters* as an example, after the multi-objective search, we achieved a series of scalable models (S, M, L) that are comparable to the state-of-the-art NAS approaches on CIFAR10/CIFAR100 datasets. Favorably, it only cost 1.3 GPU-days on NVIDIA 1080Ti, which is 1/6 of that in NSGA-Net. Since our work aims at proposing the novel NAS methods, but not the intentional design of the transferability, we do not carry out further discussion and experiments on this. Further due to the limitation of computational resources and our motivation, we do not conduct the search experiment and full training on ImageNet, and the representative experiments do not include some other non-differentiable metrics, e.g. *inference latency*. While the gaps and non-differentiable metrics issues have been addressed, an optimization approach that is based on sampling in discrete space inevitably leads to a greater computational cost. Targeting the specialized NAS scenarios, the search hyperparameters setting (reference, penalty coefficient) of each metrics is necessary, so the self-adaptive tuning of these hyperparameters is a topic worthy of research. Further, it is necessary to improve the efficiency of the search framework.

REFERENCES

- [1] Y. Guo, Y. Luo, Z. He, J. Huang, and J. Chen, "Hierarchical neural architecture search for single image super-resolution," *IEEE Signal Processing Letters*, vol. 27, pp. 1255–1259, 2020.
- [2] D. Stavroulakis, R. Ding, D. Wang, D. Lymberopoulos, B. Priyantha, J. Liu, and D. Marculescu, "Single-path mobile automl: Efficient convnet design and nas hyperparameter optimization," *IEEE Journal of Selected Topics in Signal Processing*, vol. 14, no. 4, pp. 609–622, 2020.
- [3] X. He, K. Zhao, and X. Chu, "Automl: A survey of the state-of-the-art," *Knowledge-Based Systems*, vol. 212, p. 106622, 2021.

[4] B. Zoph and Q. V. Le, "Neural architecture search with reinforcement learning," in *International Conference on Learning Representations*, 2017, pp. 1–16.

[5] X. Zheng, R. Ji, L. Tang, B. Zhang, J. Liu, and Q. Tian, "Multinomial distribution learning for effective neural architecture search," in *Proceedings of the IEEE/CVF International Conference on Computer Vision*, 2019, pp. 1304–1313.

[6] B. Zoph, V. Vasudevan, J. Shlens, and Q. V. Le, "Learning transferable architectures for scalable image recognition," in *Proceedings of the IEEE conference on computer vision and pattern recognition*, 2018, pp. 8697–8710.

[7] H. Pham, M. Y. Guan, B. Zoph, Q. V. Le, and J. Dean, "Efficient neural architecture search via parameter sharing," in *Proceedings of the 35th International Conference on Machine Learning*, 2018, pp. 4092–4101.

[8] H. Liu, K. Simonyan, and Y. Yang, "Darts: Differentiable architecture search," in *International Conference on Learning Representations*, 2019, pp. 4561–4574.

[9] A. Brock, T. Lim, J. M. Ritchie, and N. Weston, "Smash: One-shot model architecture search through hypernetworks," in *Proceedings of the international conference on learning representations*, 2018, pp. 1–22.

[10] G. Bender, P.-J. Kindermans, B. Zoph, V. Vasudevan, and Q. Le, "Understanding and simplifying one-shot architecture search," in *International Conference on Machine Learning*. PMLR, 2018, pp. 550–559.

[11] B. Lyu, Y. Yang, S. Wen, T. Huang, and K. Li, "Neural architecture search for portrait parsing," *IEEE Transactions on Neural Networks and Learning Systems*, 2021.

[12] M. Tan, B. Chen, R. Pang, V. K. Vasudevan, M. Sandler, A. Howard, and Q. V. Le, "Mnasnet:platform-aware neural architecture search for mobile," in *Proceedings of the IEEE Conference on Computer Vision and Pattern Recognition*, 2019, pp. 2820–2828.

[13] J.-D. Dong, A.-C. Cheng, D.-C. Juan, W. Wei, and M. Sun, "Dppnet: Device-aware progressive search for pareto-optimal neural architectures," in *Proceedings of the European Conference on Computer Vision (ECCV)*, 2018, pp. 540–555.

[14] C.-H. Hsu, S.-C. Chang, J.-H. Liang, H.-P. Chou, C.-H. Liu, S.-H. Chang, T. Pan, Y.-T. Chen, W. Wei, and D.-C. Juan, "Monas: Multi-objective neural architecture search using reinforcement learning," *arXiv preprint arXiv:1806.10332*, 2018.

[15] F. H. Thomas Elsken, Jan Hendrik Metzen, "Multi-objective architecture search for cnns," *arXiv preprint arXiv:1804.09081*, 2018.

[16] B. Lyu, S. Wen, K. Shi, and T. Huang, "Multiobjective reinforcement learning-based neural architecture search for efficient portrait parsing," *IEEE Transactions on Cybernetics*, 2021.

[17] Z. Lu, I. Whalen, V. Bodetti, Y. Dhebar, K. Deb, E. Goodman, and W. Banzhaf, "Nsga-net: neural architecture search using multi-objective genetic algorithm," in *Proceedings of the Genetic and Evolutionary Computation Conference*, 2019, pp. 419–427.

[18] X. Chen, L. Xie, J. Wu, and Q. Tian, "Progressive differentiable architecture search: Bridging the depth gap between search and evaluation," in *Proceedings of the IEEE/CVF International Conference on Computer Vision*, 2019, pp. 1294–1303.

[19] P. J. Angeline, G. M. Saunders, and J. B. Pollack, "An evolutionary algorithm that constructs recurrent neural networks," *IEEE transactions on Neural Networks*, vol. 5, no. 1, pp. 54–65, 1994.

[20] K. O. Stanley and R. Miikkulainen, "Evolving neural networks through augmenting topologies," *Evolutionary computation*, vol. 10, no. 2, pp. 99–127, 2002.

[21] Y. Sun, B. Xue, M. Zhang, and G. G. Yen, "Evolving deep convolutional neural networks for image classification," *IEEE Transactions on Evolutionary Computation*, vol. 24, no. 2, pp. 394–407, 2019.

[22] Y. Sun, B. Xue, M. Zhang, G. G. Yen, and J. Lv, "Automatically designing cnn architectures using the genetic algorithm for image classification," *IEEE transactions on cybernetics*, vol. 50, no. 9, pp. 3840–3854, 2020.

[23] E. Real, A. Aggarwal, Y. Huang, and Q. V. Le, "Regularized evolution for image classifier architecture search," in *Proceedings of the aaci conference on artificial intelligence*, vol. 33, no. 01, 2019, pp. 4780–4789.

[24] H. Liu, K. Simonyan, O. Vinyals, C. Fernando, and K. Kavukcuoglu, "Hierarchical representations for efficient architecture search," in *International Conference on Learning Representations*, 2017, pp. 1–13.

[25] Y. Xu, L. Xie, W. Dai, X. Zhang, X. Chen, G.-J. Qi, H. Xiong, and Q. Tian, "Partially-connected neural architecture search for reduced computational redundancy," *IEEE Transactions on Pattern Analysis and Machine Intelligence*, 2021.

[26] L. Xie, X. Chen, K. Bi, L. Wei, Y. Xu, L. Wang, Z. Chen, A. Xiao, J. Chang, X. Zhang *et al.*, "Weight-sharing neural architecture search: A battle to shrink the optimization gap," *ACM Computing Surveys (CSUR)*, vol. 54, no. 9, pp. 1–37, 2021.

[27] H. Cai, L. Zhu, and S. Han, "Proxylessnas: Direct neural architecture search on target task and hardware," in *International Conference on Learning Representations*, 2019, pp. 1–13.

[28] A. Cheng, J. Dong, C. Hsu, S. Chang, M. Sun, S. Chang, J. Pan, Y. Chen, W. Wei, and D. Juan, "Searching toward pareto-optimal device-aware neural architectures," p. 136, 2018.

[29] T. Elsken, J. H. Metzen, and F. Hutter, "Efficient multi-objective neural architecture search via lamarckian evolution," 2019.

[30] B. Lyu, H. Yuan, L. Lu, and Y. Zhang, "Resource-constrained neural architecture search on edge devices," *IEEE Transactions on Network Science and Engineering*, pp. 1–1, 2021.

[31] L. Lu and B. Lyu, "Reducing energy consumption of neural architecture search: An inference latency prediction framework," *Sustainable Cities and Society*, vol. 67, p. 102747, 2021.

[32] Z. Guo, X. Zhang, H. Mu, W. Heng, Z. Liu, Y. Wei, and J. Sun, "Single path one-shot neural architecture search with uniform sampling," in *Proceedings of the European conference on computer vision*, 2019, pp. 544–560.

[33] R. J. Williams, "Simple statistical gradient-following algorithms for connectionist reinforcement learning," *Machine Learning*, vol. 8, no. 3, pp. 229–256, 1992.

[34] Z. Gábor, Z. Kalmár, and C. Szepesvári, "Multi-criteria reinforcement learning," in *Proceedings of the 15th International Conference on Machine Learning*, 1998, pp. 197–205.

[35] S. Mannor and N. Shimkin, "A geometric approach to multi-criterion reinforcement learning," *Journal of Machine Learning Research*, pp. 325–360, 2004.

[36] V. K. Moffaert, M. M. Drugan, and A. Nowé, "Scalarized multi-objective reinforcement learning: Novel design techniques," *ADPRL*, pp. 191–199, 2013.

[37] M. Sandler, A. Howard, M. Zhu, A. Zhmoginov, and L.-C. Chen, "Mobilenetv2: Inverted residuals and linear bottlenecks," in *Proceedings of the IEEE conference on computer vision and pattern recognition*, 2018, pp. 4510–4520.

[38] B. Wu, X. Dai, P. Zhang, Y. Wang, F. Sun, Y. Wu, Y. Tian, P. Vajda, Y. Jia, and K. Keutzer, "Fbnnet: Hardware-aware efficient convnet design via differentiable neural architecture search," in *Proceedings of the IEEE/CVF Conference on Computer Vision and Pattern Recognition*, 2019, pp. 10734–10742.

[39] A. Krizhevsky, G. Hinton *et al.*, "Learning multiple layers of features from tiny images," 2009.

[40] G. Huang, Z. Liu, L. Van Der Maaten, and K. Q. Weinberger, "Densely connected convolutional networks," in *Proceedings of the IEEE conference on computer vision and pattern recognition*, 2017, pp. 4700–4708.

[41] C. Liu, B. Zoph, M. Neumann, J. Shlens, W. Hua, L.-J. Li, L. Fei-Fei, A. Yuille, J. Huang, and K. Murphy, "Progressive neural architecture search," in *Proceedings of the European conference on computer vision (ECCV)*, 2018, pp. 19–34.

[42] S. Xie, H. Zheng, C. Liu, and L. Lin, "Snas: stochastic neural architecture search," *arXiv preprint arXiv:1812.09926*, 2018.